

Luminescence properties of salts of the [Pt(4'-Ph-terpy)Cl]⁺ chromophore: crystal structure of the red form of [Pt(4'-Ph-terpy)Cl]BF₄ (4'-Ph-terpy = 4'-phenyl-2,2':6',2''-terpyridine)

Riaan Büchner,^a Corey T. Cunningham,^b John S. Field,^a Raymond J. Haines,^a David R. McMillin^b and Grant C. Summerton^a

^a Department of Chemistry, University of Natal, Pietermaritzburg, Private Bag X01, Scottsville, 3209 South Africa

^b Department of Chemistry, 1393 Brown Building, Purdue University, West Lafayette, Indiana 47907-1393, USA

Received 12th October 1998, Accepted 22nd December 1998

The complexes [Pt(4'-Ph-terpy)Cl]A (4'-Ph-terpy = 4'-phenyl-2,2':6',2''-terpyridine; A = SbF₆, CF₃SO₃, or BF₄) have been prepared by reaction of [Pt(PhCN)₂Cl₂] with the appropriate silver salt followed by addition of the 4'-phenyl-2,2':6',2''-terpyridyl ligand. The hexafluoroantimonate salt is yellow but, depending on the method of crystallisation, the triflate and tetrafluoroborate salts can be isolated in two forms, one yellow and the other red, the red forms only being stable at low temperatures. The crystal structure of red [Pt(4'-Ph-terpy)Cl]BF₄·CH₃CN has been determined at 153 K by X-ray diffraction methods. The [Pt(4'-Ph-terpy)Cl]⁺ cations are stacked face-to-face in an extended chain of stepped tetramers, with essentially equal Pt···Pt distances of *ca.* 3.3 Å within a tetramer and a Pt···Pt distance of 4.680 Å between successive tetramers. The spectroscopic and solid state emission properties of the salts have been recorded. The yellow salts are characterised by emission from an isolated chromophore in an excited state that reflects the admixture of ³MLCT (MLCT = metal-to-ligand charge-transfer) and ³IL (IL = intraligand) character. This assignment is supported by the presence of vibrational structure in the emission band as well as by a lifetime of *ca.* 1 μs for the emission. The red [Pt(4'-Ph-terpy)Cl]BF₄·CH₃CN salt, in contrast, exhibits emission from a ³MMLCT (MMLCT = metal-metal-ligand charge-transfer) state as a consequence of the strong platinum d_{x²-y²}-d_{z²} orbital interactions. This assignment is consistent with the observation of a narrow, structureless and asymmetric band as well as an emission lifetime of *ca.* 0.1 μs. There is a systematic and substantial red-shift of 75 nm in the emission maximum on cooling the red salt from 280 to 80 K, an unexpected result since bathochromic shifts of this kind are normally associated with stacked structures with a uniform Pt···Pt separation. The above assignments are further supported by measurements of the emission spectra of solutions of varying concentrations of the tetrafluoroborate salt in a dimethylformamide-methanol-ethanol glass at 77 K and by lifetime measurements. Interestingly, pressure in the form of grinding the salts modifies their luminescent properties. Thus, crushed samples of the yellow hexafluoroantimonate salt exhibit multiple emission at 80 K from both the ³MMLCT and the mixed parentage ³MLCT/³IL excited states, whereas at room temperature the emission spectrum is dominated by a broad band centred at 644 nm associated entirely with the ³MMLCT emission.

Luminescent, square-planar complexes of Pt(II) containing α,α'-diimine ligands have intriguing spectroscopic and photo-physical properties.¹ Of interest here are square-planar complexes of Pt(II) containing the 2,2':6',2''-terpyridyl (terpy) ligand, their luminescence properties being much like those of the corresponding α,α'-diimine complexes. McMillin *et al.* have reported luminescence data in fluid solution for a series of such complexes with the formula [Pt(terpy)X]⁺ where X = Cl, NCS, OMe, or OH.² Except for the chloro derivative, these chromophores exhibit broad unstructured emission signals at 25 °C in acetonitrile solution, these being assigned to a ³MLCT (MLCT = metal-ligand charge-transfer) state.² Efficient radiationless decay *via* a low-lying ³d-d state has been suggested as the reason for no detectable emission in fluid solution from the chloro derivative.² However, salts of the [Pt(terpy)Cl]⁺ cation do emit strongly in the solid state. Che *et al.* were the first to report the solid state emission spectrum of the orange-red triflate salt, this being composed of an asymmetric band centred at 600 nm at room temperature.³ At 77 K the band width decreases and the emission maximum shifts to a longer wavelength. Shifts of this type are typical of complexes of Pt(II) containing α,α'-diimine ligands in which the planar

chromophores stack uniformly in the solid, and where the d_{x²-y²} orbitals of the Pt atoms overlap to a significant extent.^{1,3,4} The solid state luminescence exhibited by materials of this type generally derives from a ³MMLCT (MMLCT = metal-metal-to-ligand charge transfer) state. More recently, Gray *et al.* have reported the solid state spectroscopy of the hexafluorophosphate, perchlorate, chloride and triflate salts of the [Pt(terpy)Cl]⁺ cation.⁵ Their results show that the colours and luminescence properties of these salts are highly dependent on the counter ion used in the precipitation, as well as on the solvent used for the crystallisation. At 77 K the emission of the various salts is assigned to a ³MMLCT transition. The room temperature solid state emission spectra were more difficult to interpret, with the luminescence exhibited by the red perchlorate salt being assigned to a ³MMLCT transition and that of the other salts to an excimeric intraligand transition resulting from π-π interactions. The temperature dependence of the solid state emission is also complicated, there either being virtually no shift in the emission maximum on lowering the temperature or a *blue* shift, in contrast to the observations made by Che and co-workers on their sample of the orange-red triflate salt.³ We have reported the temperature dependence of the emissions from the

hexafluoroantimonate and triflate salts of the $[\text{Pt}(\text{terpy})\text{Cl}]^+$ chromophore.⁶ The former salt is yellow with λ_{max} being essentially independent of temperature while our preparation of the orange-red triflate salt gave an uncorrected emission maximum at 280 K of 585 nm which shifted to a longer wavelength at 100 K, in line with the results of Che *et al.*³

We report here the photophysical properties of the hexafluoroantimonate, triflate and tetrafluoroborate salts of the $[\text{Pt}(4'\text{-Ph-terpy})\text{Cl}]^+$ ($4'\text{-Ph-terpy} = 4'\text{-phenyl-2,2':6,2''-terpyridine}$) chromophore as well as the crystal structure of the red form of the tetrafluoroborate salt. The free $4'\text{-phenyl-2,2':6,2''-terpyridyl}$ ligand is non-planar with a dihedral angle of $10.9(1)^\circ$ between the plane of the phenyl ring and that of the central pyridyl ring.⁷ Thus, the chromophore itself will be non-planar, and we wished to establish what effect this would have on the solid state structure of the salt and its luminescence properties. Che *et al.* have studied the luminescence properties of the closely related chromophores $[\text{Pt}(4'\text{R-terpy})\text{Cl}]^+$ ($\text{R} = \text{C}_6\text{H}_4\text{-OMe-}p$, $\text{C}_6\text{H}_4\text{Me-}p$, or $\text{C}_6\text{H}_4\text{CN-}p$) but only in acetonitrile solution at room temperature.³ Unlike $[\text{Pt}(\text{terpy})\text{Cl}]^+$, these chromophores exhibit ³MLCT emission in fluid solution at room temperature, and it was therefore also of interest to establish whether the $[\text{Pt}(4'\text{Ph-terpy})\text{Cl}]^+$ chromophore emits in fluid solution.

Results and discussion

Treatment of a refluxing acetonitrile solution of $[\text{Pt}(\text{PhCN})_2\text{-Cl}_2]$ with an equimolar amount of AgSbF_6 , AgCF_3SO_3 , or AgBF_4 afforded a yellow solution and a white precipitate of silver chloride. Following removal of the silver chloride, one equivalent of $4'\text{-phenyl-2,2':6,2''-terpyridine}$ ($4'\text{Ph-terpy}$) was added to afford $[\text{Pt}(4'\text{Ph-terpy})\text{Cl}]^+\text{A}^-$ ($\text{A} = \text{SbF}_6^-$, CF_3SO_3^- , or BF_4^-) which was isolated as an analytically pure and air stable yellow microcrystalline solid. A metastable red form of the triflate and tetrafluoroborate salts can also be obtained by slow evaporation of an acetonitrile solution of the compound at -10°C . Crystals grown in this manner are stable for indefinite periods when in contact with their mother-liquor at -10°C . Attempts to isolate the red triflate salt as a dry solid resulted in its immediate transformation into the more stable yellow form. However, dry crystals of the red tetrafluoroborate salt are stable for up to 6 h at -10°C and for up to 40 h when kept at liquid nitrogen temperatures, after which they slowly transform into the yellow form. The relative stability of the red tetrafluoroborate salt may be associated with the inclusion of a molecule of the solvent acetonitrile in the lattice, see below. Polymorphic behaviour of this type is now well-established for complexes of Pt(II) containing α,α' -diimine ligands and for salts of the $[\text{Pt}(\text{terpy})\text{Cl}]^+$ cation in particular.^{1,5,8}

Crystal structure of $[\text{Pt}(4'\text{Ph-terpy})\text{Cl}]\text{BF}_4 \cdot \text{CH}_3\text{CN}$

Red needle-like single crystals of $[\text{Pt}(4'\text{Ph-terpy})\text{Cl}]\text{BF}_4 \cdot \text{CH}_3\text{CN}$ were grown by dissolving the salt in acetonitrile and allowing the solvent to evaporate over a period of days at -10°C . The intensity data collection was performed at 153 K and completed within 24 h so as to prevent the transformation of the red form of the compound into its more stable yellow form. Attempts were made to grow single crystals of each of the yellow forms of the three salts prepared in this work but without success. Fig. 1 gives a perspective view of the $[\text{Pt}(4'\text{Ph-terpy})\text{Cl}]^+$ cation with the atomic numbering scheme while selected interatomic distances and angles are listed in Table 1. There are two crystallographically independent cations in the asymmetric unit the atoms of which are labelled A and B in the tables. Since there are no significant differences in the bonding parameters for cations A and B, the following discussion will be in terms of interatomic distances and angles averaged over the two cations.

Table 1 Selected interatomic distances (Å) and angles ($^\circ$) with estimated standard deviations in parentheses for $[\text{Pt}(4'\text{Ph-terpy})\text{Cl}]\text{BF}_4 \cdot \text{CH}_3\text{CN}$

Pt(A)–Cl(A)	2.296(3)	Pt(A)–N(1A)	2.008(9)
Pt(A)–N(2A)	1.929(10)	Pt–N(3A)	2.023(9)
Pt(B)–Cl(B)	2.313(3)	Pt(B)–N(1B)	2.039(9)
Pt(B)–N(2B)	1.936(9)	Pt(B)–N(3B)	2.013(10)
Cl(A)–Pt(A)–N(1A)	97.8(3)	Cl(A)–Pt(A)–N(2A)	179.4(3)
Cl(A)–Pt(A)–N(3A)	99.4(3)	N(1A)–Pt(A)–N(2A)	82.2(3)
N(1A)–Pt(A)–N(3A)	162.8(4)	N(2A)–Pt(A)–N(3A)	80.7(4)
Cl(B)–Pt(B)–N(1B)	99.1(3)	Cl(B)–Pt(B)–N(2B)	179.8(2)
Cl(B)–Pt(B)–N(3B)	99.3(3)	N(1B)–Pt(B)–N(2B)	81.0(4)
N(1B)–Pt(B)–N(3B)	161.7(4)	N(2B)–Pt(B)–N(3B)	80.7(4)

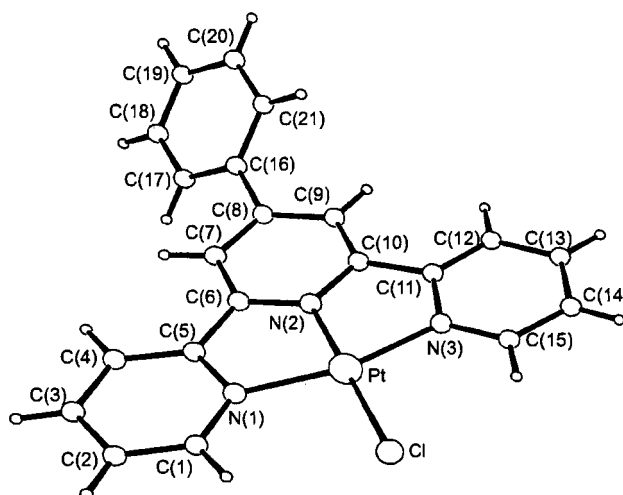


Fig. 1 Perspective view of the $[\text{Pt}(4'\text{Ph-terpy})\text{Cl}]^+$ cation.

As expected, the coordination geometry of the platinum atom is essentially square-planar, deviations from the idealised geometry being largely a consequence of the geometric constraints imposed by the $4'\text{-phenyl-2,2':6,2''-terpyridyl}$ ligand. Thus, the $\text{N}(1)\text{-Pt-N}(2)$ and $\text{N}(2)\text{-Pt-N}(3)$ angles of $81.6(3)$ and $80.7(3)^\circ$ are less than 90° , whereas the $\text{N}(1)\text{-Pt-Cl}$ and $\text{N}(3)\text{-Pt-Cl}$ angles of 98.5 and 99.3° are greater than 90° . The Pt–N distances show the normal variation with that to the bridgehead nitrogen atom being *ca.* 0.09 \AA shorter than those to the two outer nitrogen atoms. Indeed, the N–Pt–N angles and Pt–N distances are in excellent agreement with those previously reported for terpyridyl complexes of Pt(II).^{5,6,9} The Pt–Cl distance of $2.305(2) \text{ \AA}$ is very similar to those reported for $[\text{Pt}(\text{terpy})\text{Cl}]\text{CF}_3\text{SO}_3$ and $[\text{Pt}(\text{terpy})\text{Cl}]\text{ClO}_4$ these being 2.307 and 2.302 \AA respectively.^{3,5} The cation as a whole is non-planar because of a twist about the interannular bond $[\text{C}(8)\text{-C}(16)]$ that results in a dihedral angle between the planes of the phenyl and central pyridyl rings of $33.4(1)^\circ$. In the case of the free $4'\text{-phenyl-2,2':6,2''-terpyridyl}$ ligand the corresponding angle is $10.9(1)^\circ$. As noted by Constable *et al.*,⁷ the latter angle is adopted in order to minimise non-bonded $\text{H}\cdots\text{H}$ repulsions between the *ortho* protons of the phenyl ring and the $\text{H}_{3,5}$ protons of the terpyridyl ligand while, at the same time, maximising π -conjugation between the phenyl and terpyridyl ring system. It is not clear why a considerably larger dihedral angle is observed for the complex but the effect appears real, as a very similar twist about the interannular bond of $33.5(1)^\circ$ was observed for the $4'\text{-phenyl-2,2':6,2''-terpyridyl}$ ligand in $[\text{Pt}(4'\text{Ph-terpy})(\text{C}\equiv\text{CPh})]\text{SbF}_6$.¹⁰ Electronic effects associated with the coordination of the terpyridyl unit to the platinum atom are probably the most important, but crystal packing effects may also play a role, at least for the red tetrafluoroborate salt, see below.

Fig. 2 depicts the packing architecture observed for $[\text{Pt}(4'\text{Ph-terpy})\text{Cl}]\text{BF}_4 \cdot \text{CH}_3\text{CN}$. The $[\text{Pt}(4'\text{Ph-terpy})\text{Cl}]^+$ cations are

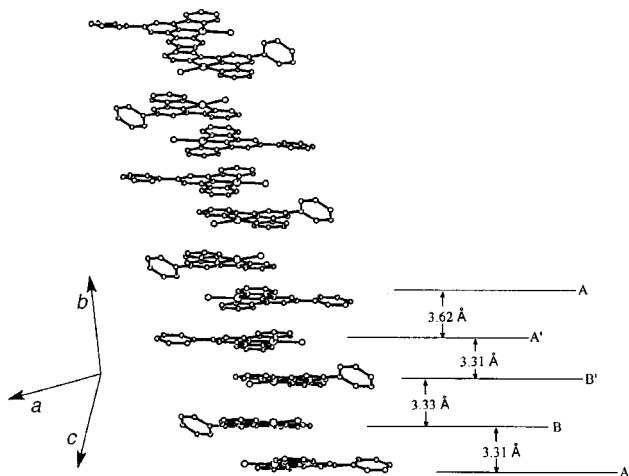


Fig. 2 Stacking of the $[\text{Pt}(4'\text{-Ph-terpy})\text{Cl}]^+$ cations in $[\text{Pt}(4'\text{-Ph-terpy})\text{Cl}]\text{BF}_4 \cdot \text{CH}_3\text{CN}$.

stacked in an extended chain of stepped tetramers parallel to the b axis. Each tetramer consists of two pairs of crystallographically independent cations, one pair (labelled A and B) being related to the second pair (labelled A' and B') by a centre of inversion halfway up the b axis. The independent cations A and B are effectively parallel as evidenced by a dihedral angle of only $0.1(1)^\circ$ between the mean planes through the Pt atom and the atoms comprising the terpyridyl unit of each cation. As far as the interplanar spacings within the tetramer are concerned, that between the crystallographically independent cations is 3.31 \AA , while that between adjacent centre of symmetry related cations is 3.33 \AA (see Fig. 2). The equivalent Pt...Pt distances within the tetramer are $3.303(3)$ and $3.333(3) \text{ \AA}$. The differences of 0.02 \AA in the interplanar spacings and 0.03 \AA in the Pt...Pt distances are not pronounced, and thus the stacking within a tetramer is essentially uniform. However, the interplanar spacing and Pt...Pt distance involving the peripheral cations of successive tetramers of 3.62 and 4.680 \AA respectively are significantly longer and, as such, define the boundary between consecutive tetramers within the extended chain. The relatively large difference between the latter two distances reflects the extent of slippage of the tetramers with respect to each other; it is in this sense that the chain of tetramers is described as "stepped". In terms of possible bonding interactions between the chromophores the interplanar separations of *ca.* 3.3 \AA are less than 3.8 \AA , the upper distance limit for π -interactions between organic species,¹¹ suggesting that there could be a significant π -interaction between the chromophores making-up any one tetramer. The Pt...Pt distances of *ca.* 3.3 \AA are very similar to values normally taken to indicate a strong σ -interaction between overlapping platinum d_z^2 orbitals.¹ That the platinum atoms are correctly positioned for effective end-on overlap of the d_z^2 orbitals, is evidenced by the fact that the platinum atoms of successive chromophores within a tetramer are almost eclipsed, when viewed perpendicular to the planes of the stacked cations. However, the between tetramer interplanar spacing (3.62 \AA) and Pt...Pt distance (4.680 \AA) are too large on one hand, and the extent of slippage between adjacent tetramers too great on the other, to support significant bonding interactions between tetramers.

The crystal packing motif described above for $[\text{Pt}(4'\text{-Ph-terpy})\text{Cl}]\text{BF}_4 \cdot \text{CH}_3\text{CN}$ is not typical of stacked complexes of Pt(II) containing α, α' -diimine ligands in general. More common structural types for these complexes are: *linear chain structures* in which there is a single Pt...Pt distance that is constant along an infinite linear chain; and *dimer* structures in which the platinum complexes segregate into pairs.¹ More specifically, Connick *et al.* have shown that the Pt...Pt distance in a linear chain structure is determined by a subtle interplay of electronic

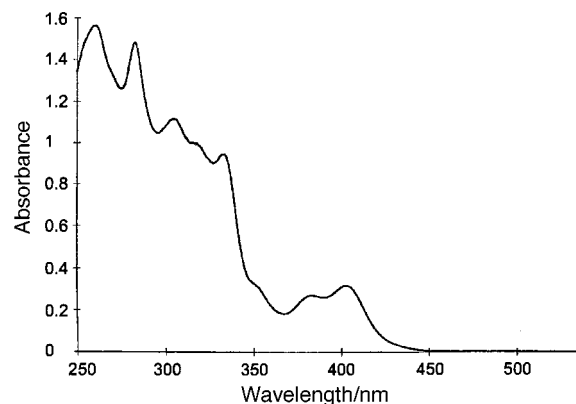


Fig. 3 Absorption spectrum of $[\text{Pt}(4'\text{-Ph-terpy})\text{Cl}]\text{SbF}_6$ in acetonitrile.

effects associated with the diimine ligand.¹² With regard to salts of the $[\text{Pt}(\text{terpy})\text{Cl}]^+$ cation, the crystal structure of the perchlorate salt consists of discrete Pt_2 units arranged along an infinite terpyridyl π -stack,⁵ whereas the triflate structure is more appropriately described as discrete dimers in both Pt...Pt and terpy...terpy interactions.³ Similar to $[\text{Pt}(\text{terpy})\text{Cl}]\text{ClO}_4$, the 4'-phenyl-2,2':6',2''-terpyridyl ligand complex $[\text{Pt}(4'\text{-Ph-terpy})\text{Cl}]\text{SbF}_6$ crystallises in discrete Pt_2 dimers along a uniform π -stack.¹⁰ It is clear that the precise stacking motif adopted by a platinum(II) complex containing the terpyridyl or a substituted terpyridyl ligand is sensitive to a number of factors such as: the degree of planarity of the 4'-R-terpyridyl (R = H, Ph, *etc.*) ligand, the steric requirements of the fourth ligand bonded to platinum, the size of the counter ion (assuming the complex is ionic), the method of crystallisation and the temperature.

Electronic spectroscopy and photophysics of $[\text{Pt}(4'\text{-Ph-terpy})\text{Cl}]\text{A}$ (A = SbF_6 , CF_3SO_3 , or BF_4)

The room temperature absorption spectrum of $[\text{Pt}(4'\text{-Ph-terpy})\text{Cl}]\text{SbF}_6$ measured in acetonitrile is shown in Fig. 3, that of the other salts prepared in this work being identical. The peak pattern and the wavelengths of the peak maxima are similar to those recorded in acetonitrile by McMillin *et al.* and by Che *et al.* for the $[\text{Pt}(\text{terpy})\text{Cl}]^+$ chromophore.^{2,3} On this basis the peak at 283 nm ($\epsilon = 31\,419 \text{ mol}^{-1} \text{ dm}^3 \text{ cm}^{-1}$) as well as the vibrationally structured band between 300 and 350 nm are assigned to $^1(\pi-\pi^*)$ transitions associated with the coordinated 4'-phenylterpyridine ligand. The bands with $\lambda(\text{abs})_{\text{max}}$ greater than 350 nm can be assigned to MLCT transitions based on the similarity of their relative intensities and wavelengths to those of the analogous bands measured in acetonitrile for the $[\text{Pt}(\text{terpy})\text{Cl}]^+$, $[\text{Pt}(\text{terpy})\text{OH}]^+$ and $[\text{Pt}(\text{terpy})\text{NCS}]^+$ chromophores.²

Emission from fluid solutions of the $[\text{Pt}(4'\text{-Ph-terpy})\text{Cl}]\text{A}$ salts in acetonitrile and dichloromethane is vanishingly weak. This is typical of square-planar complexes of Pt(II) and has been attributed to the presence of low-lying d-d excited states that are unstable with respect to D_{2d} distortions, this being likely to facilitate non-radiative decay.² However, emission from solid samples of the salts is strong and, moreover, temperature dependent. The emission characteristics of the yellow hexafluoroantimonate salt as well as of the yellow forms of the dimorphic triflate and tetrafluoroborate salts are virtually identical. On the other hand, the only red salt stable enough for its emission spectra to be measured is that containing the tetrafluoroborate anion. For these reasons, the emission spectra recorded for the yellow and red forms of $[\text{Pt}(4'\text{-Ph-terpy})\text{Cl}]\text{BF}_4$ form the basis of the following discussion of luminescence properties.

Fig. 4 shows the solid state emission spectra of the yellow form of $[\text{Pt}(4'\text{-Ph-terpy})\text{Cl}]\text{BF}_4$ recorded at 40 K intervals over

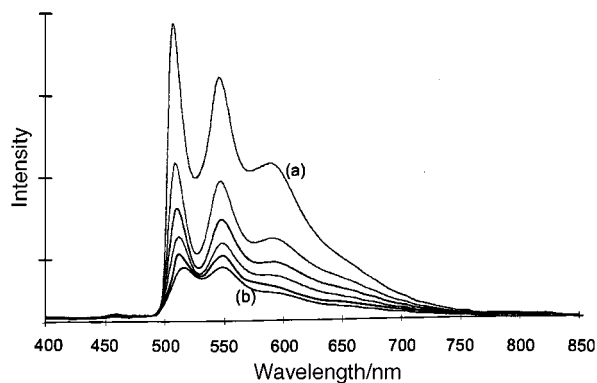


Fig. 4 Solid state emission spectrum of $[\text{Pt}(4'\text{Ph-terpy})\text{Cl}]\text{BF}_4$ (yellow form) recorded at 40 K intervals over the range 80 (a) to 280 K (b). $\lambda_{\text{ex}} = 340$ nm.

the temperature range 80–280 K. The dominant feature is a vibrationally structured band with three components, these occurring at 518, 552 and 590 nm at 80 K. The spacing between the 0–0 and 0–1 transitions is 1200 cm^{-1} , and the Huang–Rhys factor defined as I_{0-1}/I_{0-0} is *ca.* 0.8, characteristic of emission from either a $\pi\text{-}\pi^*$ ($4'\text{Ph-terpy}$) or $d(\text{Pt})\text{-}\pi^*(4'\text{Ph-terpy})$ charge transfer excited state.^{1,13} However, closer examination of the emission spectra in Fig. 4 reveals the presence of a further weak, but discernable band at *ca.* 466 nm. This band is reminiscent of the 0–0 transition observed at 465 nm in the vibrationally structured emission spectrum of $[\text{Pt}(\text{terpy})\text{Cl}]\text{CF}_3\text{SO}_3$ recorded in a dilute butyronitrile glass at 77 K.³ It is also similar to the shortest wavelength transition in the structured emission that Gray and co-workers observed for $\{[\text{Pt}(\text{terpy})_2(\mu\text{-Hpz})]\}^{3+}$ (Hpz = pyrazole) in a 1:10:10 DME–ethanol–methanol glass at 77 K.¹⁴ Emission in both these cases was assigned to occur from an intraligand ${}^3(\pi\text{-}\pi^*)$ excited state.^{3,14} Thus, the emission with its origin at 518 nm is red-shifted with respect to emission from a “pure” intraligand state, which probably reflects that the excited state contains both $\pi\text{-}\pi^*$ and $d\text{-}\pi^*$ character *i.e.* it is of the $(d,\pi)\text{-}\pi^*$ type recently reported as the emitting state in fluid solution for salts of the $[\text{Pt}(4'\text{R-terpy})\text{Cl}]^+$ chromophore, where R is the electron-donating substituent SMe or NMe_2 .¹⁵ Such an assignment is consistent with the $[\text{Pt}(4'\text{R-terpy})\text{Cl}]^+$ chromophores being in a monomeric environment in the crystal as, indeed, is the absence of any shift in the *positions* of the bands on lowering the temperature (Fig. 4). There is, however, an increase in the intensities of the bands on lowering the temperature implying that there is a thermally activated non-radiative decay pathway that becomes less significant at reduced temperatures. The emission decay observed at both room temperature and 77 K was not monoexponential, the emission lifetime in the tail of the decay curve being about 0.9 and 5 μs respectively. These lifetimes suggest that the emission originates from a state of triplet multiplicity.

Fig. 5 shows the solid state emission spectra of the metastable red form $[\text{Pt}(4'\text{Ph-terpy})\text{Cl}]\text{BF}_4\cdot\text{CH}_3\text{CN}$, recorded at 40 K intervals over the temperature range 80–280 K. In stark contrast to the vibrationally structured emission spectrum of the yellow form, the emission spectrum of the red form at 280 K exhibits an asymmetric peak centred at 655 nm that is devoid of any vibrational structure; the peak is also narrow with a full-width-at-half-maximum (fwhm) value of 1290 cm^{-1} . Lowering the temperature to 80 K results in a substantial red shift in the emission maximum to 730 nm and a further narrowing of the peak (fwhm = 990 cm^{-1}). Band profiles and red shifts of the above type are typical of the emission spectra of polypyridyl complexes of platinum(II) with linear chain structures, as observed for the triflate³ and tetrafluoroborate⁶ salts of the $[\text{Pt}(\text{terpy})\text{Cl}]^+$ chromophore and the 2,2'-bipyridyl (bipy) ligand complex $[\text{Pt}(\text{bipy})\text{Cl}_2]$,^{1,16} for example. These salts exhibit

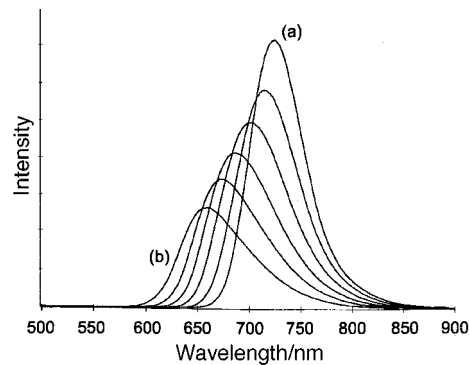


Fig. 5 Solid state emission spectrum of $[\text{Pt}(4'\text{Ph-terpy})\text{Cl}]\text{BF}_4\cdot\text{CH}_3\text{CN}$ (red form) recorded at 40 K intervals over the range 80 (a) to 280 K (b). $\lambda_{\text{ex}} = 340$ nm.

$\pi^*(\text{terpy}) \longrightarrow d\sigma^*$ emissions from MMLCT excited states, the characteristic red-shift in the emission maximum being due to a decrease in the mean $\text{Pt}\cdots\text{Pt}$ spacing when the temperature is lowered, as has been shown to occur for the red form of $[\text{Pt}(\text{bipy})\text{Cl}_2]$ by means of crystal structure determinations at 294 and 20 K.¹⁷ As already noted, $[\text{Pt}(4'\text{Ph-terpy})\text{Cl}]\text{BF}_4\cdot\text{CH}_3\text{CN}$ does not have a linear chain structure, in that there is not a uniform $\text{Pt}\cdots\text{Pt}$ spacing along the entire stack, at least not at 153 K. However, the temperature dependence of the emission spectrum strongly suggests that the emitting state is MMLCT and that the $\text{Pt}\cdots\text{Pt}$ distances within a tetramer decrease due to lattice contraction on lowering the temperature. Despite earlier suggestions,⁵ it therefore appears that it is *not* necessary to have an infinite chain structure with uniform $\text{Pt}\cdots\text{Pt}$ separations in order to observe a systematic red-shift in the emission maximum on lowering the temperature. What is certain is that the intratetramer $\text{Pt}\cdots\text{Pt}$ distances of *ca.* 3.3 \AA measured at 153 K, are sufficiently short to allow for a substantial $d_z\text{-}d_z$ orbital interaction,¹⁸ consistent with the assignment of the lowest excited state as being MMLCT in origin. Similar to that observed for the yellow salt, there is a progressive increase in the emission intensity on lowering the temperature, associated with the presence of a thermally activated non-radiative pathway that becomes less significant at lower temperatures. The emission decay is essentially monophasic both at room temperature and at 77 K, the lifetimes being about 90 and 1100 ns respectively, again consistent with emission from a state of triplet multiplicity.

Clearly, the crystal structures of the yellow and red forms of the tetrafluoroborate salt determine their solid state emission properties. In the case of the yellow form, the $[\text{Pt}(4'\text{Ph-terpy})\text{Cl}]^+$ chromophore appears to be in a monomeric environment, whereas $\text{Pt}\cdots\text{Pt}$ interactions are responsible for the emission characteristics of the red salt. As noted by Miskowski and Houlding,¹⁹ comparison of the solid state emission spectra with those recorded in the glassy state, can provide information on the influence of solid state interactions on the electronic structure of the chromophore and, in particular, on whether the $[\text{Pt}(4'\text{Ph-terpy})\text{Cl}]^+$ chromophore is in a monomeric environment in crystals of the yellow salt. Accordingly, the emission spectra of butyronitrile glasses containing varying concentrations of $[\text{Pt}(4'\text{Ph-terpy})\text{Cl}]\text{BF}_4$ at 77 K were recorded, the results being shown in Fig. 6. The emission spectrum observed for the most dilute glass (0.005 mM) is very similar to that observed in the solid state at 80 K for the yellow salt (Fig. 4), including the appearance of a small feature on the high energy side of the spectrum centred at 466 nm. However, the dominant emission maxima at 505, 540 and 580 nm are slightly blue-shifted with respect to those recorded for the yellow solid at 80 K, which may reflect the presence of a π -stacking interaction in the dilute glass. If so, aggregates of this type must be small *e.g.* dimers. On balance and as for the yellow solid, a mixed parent-

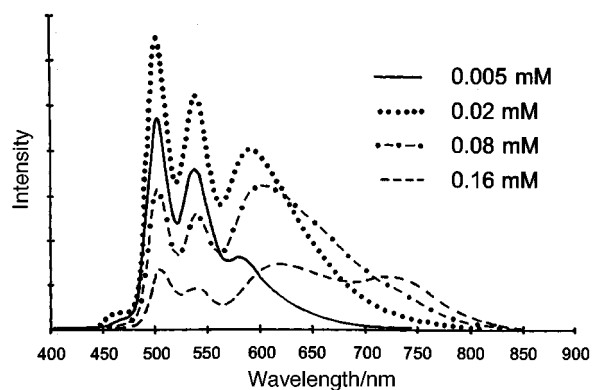


Fig. 6 The emission spectrum of a 77 K butyronitrile glass of $[\text{Pt}(4'\text{Ph-terpy})\text{Cl}]\text{BF}_4$ (yellow form) recorded over the concentration range 0.005 to 0.160 mM. $\lambda_{\text{ex}} = 340$ nm.

age assignment *i.e.* $^3[(d,\pi)-\pi^*]$ is preferred.¹⁵ On increasing the concentration, the 466 nm band gradually disappears; the positions of the first two major high energy bands remain unchanged, though their overall intensities do vary reaching a minimum at the highest concentration of 0.160 mM; and the low energy band at 580 nm begins to broaden, until at the highest concentration of 0.160 mM two broad and unstructured bands of higher intensity and centred at 622 and 726 nm are clearly visible (Fig. 6). The position of the latter band coincides with that recorded in the solid state at 80 K for red $[\text{Pt}(4'\text{Ph-terpy})\text{Cl}]\text{BF}_4 \cdot \text{CH}_3\text{CN}$. Thus, at higher concentrations different aggregates of the $[\text{Pt}(4'\text{Ph-terpy})\text{Cl}]^+$ chromophore form that involve significant $\text{Pt} \cdots \text{Pt}$ interactions giving rise to the change in bandshape and the red-shift in the emission. Most likely, the emission maximum at 726 nm observed for the 0.160 mM butyronitrile glass solution derives from a $^3\text{MMLCT}$ state. Assignment of the broad midrange band centred at 622 nm is less straightforward. Similar luminescence in the range 550–650 nm has been observed at 77 K for a concentrated glassy solution of $[\text{Pt}(\text{terpy})\text{Cl}]\text{PF}_6$ in DME.⁵ The authors proposed that such broad luminescence could be a consequence of emissions from dimeric structures in which both 4'Ph-terpy $\pi-\pi$ and platinum d_z-d_z interactions are important. As such, the broad emission observed at 622 nm probably has both $\pi\pi$ excimer and $^3\text{MMLCT}$ character.

Interestingly, the solid state luminescent behaviour of the yellow hexafluoroantimonate salt and the yellow forms of the triflate and tetrafluoroborate salts, changes on crushing and grinding the sample. In particular, the colour of the luminescence at room temperature changes from bright yellow to bright orange, as perceived by the eye when the sample is held under a blanket of ultraviolet radiation. Cooling such a crushed sample to liquid nitrogen temperatures resulted in the colour of the luminescence changing back to the original yellow. Further heating/cooling cycles revealed that this temperature dependent change in the colour of the luminescence is completely reversible. However, crushing has no visible effect on the yellow colour of the sample. This behaviour was observed for a large number of different sample preparations and so must be considered reproducible. In order to investigate further the temperature dependence of the emission from crushed samples of the yellow salts the emission spectra from a crushed sample of $[\text{Pt}(4'\text{Ph-terpy})\text{Cl}]\text{SbF}_6$ were recorded over the temperature range 80 to 280 K, the results being shown in Fig. 7. The 280 K spectrum consists of a broad unstructured band centred at 644 nm that is similar in profile and position to the band observed in the emission spectrum recorded at 280 K for the red polymorph of the tetrafluoroborate salt, the only significant differences being a blue shift of *ca.* 11 nm in the emission maximum and a broadening of the peak (*cf.* Figs. 5 and 7). On decreasing the temperature there is an increase in the intensity as well as a red shift in the position of this band.

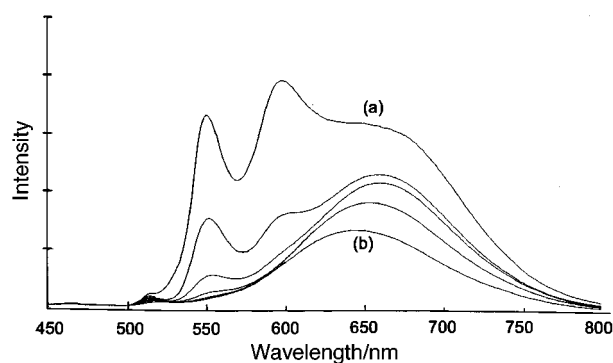


Fig. 7 The solid state emission spectrum of a crushed sample of $[\text{Pt}(4'\text{Ph-terpy})\text{Cl}]\text{SbF}_6$ recorded at 80 K (a), 130 K, 160 K, 220 K and 280 K (b). $\lambda_{\text{ex}} = 340$ nm.

Again, this behaviour is reminiscent of that observed when samples of red $[\text{Pt}(4'\text{Ph-terpy})\text{Cl}]\text{BF}_4 \cdot \text{CH}_3\text{CN}$ are cooled (Fig. 5). A more significant change in the emission spectrum brought about by cooling the sample to 80 K is the development of two well-resolved and relatively intense high energy bands at 554 and 595 nm. The latter coincide with the two low energy vibrational bands observed in the emission spectrum of the yellow tetrafluoroborate salt (Fig. 4) but have different relative intensities. The vibrational feature at 518 nm in the emission spectrum of the yellow tetrafluoroborate salt has as its counterpart a weak band at *ca.* 520 nm in the room temperature emission spectrum of the crushed sample. These differences in relative intensities of the high energy bands may be attributed, at least in part, to the presence of the strong and overlapping low energy band. Three conclusions may be drawn from the above data. (i) At 280 K emission by the crushed sample is largely *via* radiative decay from a $^3\text{MMLCT}$ excited state. (ii) At 80 K simultaneous emission occurs both from a $^3\text{MMLCT}$ and a $^3[(d,\pi)-\pi^*]$ state. (iii) The lower energy $^3\text{MMLCT}$ state is almost exclusively populated at 280 K whereas both states are significantly populated at low temperatures. It would seem that crushing the yellow hexafluoroantimonate salt forces the $[\text{Pt}(4'\text{Ph-terpy})\text{Cl}]^+$ chromophores closer together in a stacked configuration such that $\text{Pt} \cdots \text{Pt}$ interactions become important. A $^3\text{MMLCT}$ state enters the excited state manifold along with the $^3[(d,\pi)-\pi^*]$ state. Given sufficient thermal energy, vibronic interactions allow these two states to couple and interconversion between them occurs. As expected, the lower energy $^3\text{MMLCT}$ state is almost exclusively populated at higher temperatures. Temperature dependent multiple emission of this type has been observed for $[\text{Cu}(2,9\text{-Me}_2\text{-1,10-phen})(\text{PPh}_3)_2]^+$ (1,10-phen = 1,10-phenanthroline) in fluid solution, which has also been explained on the basis of multiple emission from vibronically coupled excited states.²⁰ However, there are two other possible models bearing in mind that we are dealing here with multiple emission in the *solid* state. For instance, the emission could come from spatially distinct centres in the solid.²¹ In this view, the energy migrates (at higher temperatures) from bulk sites to defect sites where the $\text{Pt} \cdots \text{Pt}$ interactions are significant. However, energy migration slows down at low temperatures so we see bulk emission. Since the material is yellow, the defects have to be few and far between. Alternatively, any given excited state in the bulk may re-arrange to form a short $\text{Pt} \cdots \text{Pt}$ interaction which then emits. At low temperatures the rearrangement process becomes impossible. In this view, the excited state either rearranges or it does not, and there is no need to postulate rapid energy transfer. Again, the colour is yellow, because the $\text{Pt} \cdots \text{Pt}$ dimer is only a transient. Similar arguments have been used to explain otherwise unexpected differences in the temperature dependence of the solid state emission spectra of various salts of the $[\text{Pt}(\text{terpy})\text{Cl}]^+$ chromophore.⁶

Conclusion

The solid state luminescence properties of salts of the [Pt(4'-Ph-terpy)Cl]⁺ chromophore depend on the choice of counter ion, in this case BF₄⁻, CF₃SO₃⁻, or SbF₆⁻. The size of the counter ion determines the arrangement of the cations in the solid and, in particular, whether the chromophores exist in a monomeric environment or in a stacked configuration with significant interactions between the platinum d_{z²} orbitals. Also important is the method of crystallisation, since the triflate and tetrafluoroborate salts can be isolated in a yellow and a red form. The yellow salts typically exhibit emission from a ³[(d,π)-π*] excited state, indicative of the chromophore being in a monomeric environment. Such an assignment is supported by the presence of vibrational structure in the emission band and by a lifetime of ca. 1 μs for the emission. The crystal structure of the red [Pt(4'-Ph-terpy)Cl]BF₄·CH₃CN salt at 153 K shows the cations to be stacked face-to-face in an extended chain of tetramers, with significant platinum d_{z²}-d_{z²} orbital interactions within a tetramer, but only non-bonding interactions between tetramers. Emission is from a ³MMLCT excited state as a consequence of the strong interactions between the platinum d_{z²} orbitals within a tetramer. In this case the assignment is consistent with the observation of a narrow (fwhm = 1290 cm⁻¹) structureless and asymmetric band as well as with an emission lifetime of ca. 0.1 μs. There is a systematic red-shift in the emission maximum on lowering the temperature, an effect usually only associated with linear chain structures with uniform Pt···Pt separations. We have also observed an interesting and reproducible effect of pressure on the crystal structure and associated luminescence properties of the yellow salts, this behaviour being exemplified by a study of the dependence on temperature of emission from crushed samples of the hexafluoroantimonate salt. Thus, crushed samples of [Pt(4'-Ph-terpy)Cl]SbF₆ exhibit emission from a ³MMLCT state at room temperature and simultaneous emission from both ³MMLCT and ³[(d,π)-π*] states at low temperatures such as 80 K; interestingly the effect of temperature is reversible.

Experimental

Materials and instruments

Dichlorobis(benzonitrile)platinum(II) was obtained from Strem Chemicals and the silver salts AgA (A = SbF₆, CF₃SO₃, or BF₄) from Fluka AG and used without further purification. The 4'-phenyl-2,2':6',2''-terpyridyl ligand was prepared by the method of Constable *et al.*⁷ Acetonitrile was purified by the method of Carlsen and Anderson;²² other solvents were dried over standard reagents and distilled prior to use.²³ The C, H and N analyses were performed using an in-house Perkin-Elmer 2400 Elemental Analyser. Infrared spectra were recorded on a Shimadzu FTIR-4300 spectrometer as KBr discs. UV-vis absorption spectra were recorded in deoxygenated solvents using a Shimadzu UV-2101PC Scanning Spectrophotometer. Solid state emission spectra were recorded on microcrystalline samples using a SLM-Aminco SPF 500C fluorimeter. For the variable temperature emission measurements the cryostat was an Oxford Instruments DN1704 liquid-nitrogen-cooled system complete with an Oxford Instruments temperature controller. The excitation wavelength was usually 340 nm, the scattered light being removed by a 400 nm long-wave-pass filter. The 337 nm line from a nitrogen laser served as the excitation source for the lifetime measurements, a 337 nm band pass filter being used to remove stray light from the beam. Lifetime data were analysed as described previously.²⁴

Synthesis

[Pt(4'-Ph-terpy)Cl]A (A = SbF₆, CF₃SO₃, or BF₄). To a suspension of [PtCl₂(PhCN)₂] (0.100 g, 0.210 mmol) in CH₃CN

Table 2 Summary of crystal data and structure determination for [Pt(4'-Ph-terpy)Cl]BF₄·CH₃CN

Formula	C ₂₃ H ₁₈ BClF ₄ N ₄ Pt
<i>M</i>	667.75
<i>T</i> /K	153
Crystal size/mm	0.70 × 0.20 × 0.16
Crystal system	Triclinic
Space group	<i>P</i> $\bar{1}$
<i>a</i> /Å	12.613(5)
<i>b</i> /Å	13.697(5)
<i>c</i> /Å	14.560(5)
<i>a</i> ^o	71.11(1)
<i>β</i> ^o	85.65(1)
<i>γ</i> ^o	72.32(1)
<i>U</i> /Å ³	2266.7(8)
<i>Z</i>	4
<i>D</i> _c /g cm ⁻³	1.956
<i>μ</i> /mm ⁻¹	6.686
<i>F</i> (000)	1304
Reflections measured	6793
Unique reflections	5629
Reflections with <i>F</i> ² ≥ 2σ(<i>F</i> ²)	4520
Transmission	0.498 to 0.927
<i>R</i> _{int}	0.0236
Weighting parameters ^a <i>a</i> , <i>b</i>	0.0720, 0
<i>R</i> [<i>F</i> ² ≥ 2σ(<i>F</i> ²)] ^b	0.0444
<i>wR</i> 2 [all data] ^c	0.1175
Number of refined parameters	613
Goodness of fit ^d	1.036
Maximum, minimum electron density/e Å ⁻³	1.441, -2.209

^a *w*⁻¹ = σ(*F*_o²) + (*aP*)² + *bP*, where *P* = (*F*_o² + 2*F*_c²)/3. ^b *R* = Σ|*F*_o| - |*F*_c|/Σ|*F*_o|. ^c *wR*2 = [Σ*w*(*F*_o² - *F*_c²)²/Σ*w*(*F*_o²)²]^{1/2}. ^d *S* = [Σ*w*(*F*_o² - *F*_c²)²/(no. of unique reflections - no. of variables)]^{1/2}.

(10 cm³) was added an equimolar amount of AgA (0.072 g for A = SbF₆; 0.054 g for A = CF₃SO₃; and 0.041 g for A = BF₄) dissolved in CH₃CN (5 cm³). The reaction mixture was heated under reflux for 16 h, the precipitated AgCl removed by filtration and one equivalent of solid 4'-phenyl-2,2':6',2''-terpyridine (0.066 g, 0.210 mmol) added. The mixture was refluxed for a further 24 h, following which the volume of the solution was reduced *in vacuo* resulting in the precipitation of [Pt(4'-Ph-terpy)Cl]A as a yellow microcrystalline solid. This was filtered off, washed with diethyl ether and dried *in vacuo*. Yield ca. 75% (A = SbF₆, found: C, 32.6; H, 2.0; N, 5.6. C₂₁H₁₅ClF₆N₃PtSb requires C, 32.5; H, 2.0; N, 1.4%. A = CF₃SO₃, found: C, 38.4; H, 2.1; N, 6.1. C₂₂H₁₅ClF₃N₃O₃PtS requires C, 38.4; H, 2.1; N, 6.1%. A = BF₄, found: C, 40.3; H, 2.3; N, 6.9. C₂₁H₁₅BClF₄N₃Pt requires C, 40.2; H, 2.4; N, 6.7%). IR (KBr): ν(4'-Ph-terpy) 1612s, 1560m, 1480m, 1418m, 890w; ν(SbF₆⁻) 656vs; ν(CF₃-SO₃⁻) 1266vs, 1174m, 1030m; ν(BF₄⁻) 1053vs (br) cm⁻¹.

Crystallography

A suitable crystal of [Pt(4'-Ph-terpy)Cl]BF₄·CH₃CN was quickly transferred from the mother-liquor to a stream of cold nitrogen at 153 K on a Siemens SMART diffractometer fitted with a CCD-type area detector, and data were collected at 153 K. Graphite-monochromatised Mo-*K*α radiation was used. Absorption corrections were applied using SADABS.²⁵ Details of the crystal data, data collection and structure refinement are given in Table 2.

The structure was solved using conventional heavy atom and Fourier methods and refined by the full-matrix least-squares method on all *F*² data using the program SHELX-93.²⁶ Non-hydrogen atoms were refined with anisotropic thermal parameters; hydrogen atoms were included in calculated positions and refined with isotropic thermal parameters riding on those of the parent atom.

CCDC reference number 186/1303.

See <http://www.rsc.org/suppdata/dt/1999/711/> for crystallographic files in .cif format.

Acknowledgements

We thank the University of Natal and the South African Foundation for Research Development for financial support. Our grateful thanks go to Leanne Cook for the X-ray intensity data collection.

References

- 1 V. H. Houlding and V. M. Miskowski, *Coord. Chem. Rev.*, 1991, **111**, 145.
- 2 T. K. Aldridge, E. M. Stacey and D. R. McMillin, *Inorg. Chem.*, 1994, **33**, 722.
- 3 H.-K. Yip, L.-K. Cheung, K.-K. Cheung and C.-M. Che, *J. Chem. Soc., Dalton Trans.*, 1993, 2933.
- 4 V. M. Miskowski and V. H. Houlding, *Inorg. Chem.*, 1991, **30**, 4446.
- 5 J. A. Bailey, M. G. Hill, R. E. Marsh, V. M. Miskowski, W. P. Schaefer and H. B. Gray, *Inorg. Chem.*, 1995, **34**, 4591.
- 6 R. Büchner, J. S. Field, R. J. Haines, C. T. Cunningham and D. R. McMillin, *Inorg. Chem.*, 1997, **37**, 3952.
- 7 E. C. Constable, J. Lewis, M. C. Liptrot and P. R. Raithby, *Inorg. Chim. Acta*, 1990, **178**, 47.
- 8 R. S. Osborn and D. Rogers, *J. Chem. Soc., Dalton Trans.*, 1974, 1002; E. Bielli, P. M. Gidney, R. D. Gilliard and B. T. Heaton, *ibid.*, 1974, 2133.
- 9 K. W. Jennette, J. T. Gill, J. A. Sadowick and S. J. Lippard, *J. Am. Chem. Soc.*, 1976, **98**, 6159; M. Akiba, K. Umakoshi and Y. Sasaki, *Chem. Lett.*, 1995, 607; J. A. Bailey, V. M. Miskowski and H. B. Gray, *Acta Crystallogr., Sect. C*, 1992, **48**, 1420.
- 10 R. Büchner, PhD Thesis, University of Natal, Pietermaritzburg, 1996.
- 11 D. P. Freyburg, J. L. Robins, K. N. Raymond and J. C. Smart, *J. Am. Chem. Soc.*, 1979, **101**, 892.
- 12 W. B. Connick, R. E. Marsh, W. P. Schaefer and H. B. Gray, *Inorg. Chem.*, 1997, **36**, 913.
- 13 V. M. Miskowski, V. H. Houlding, C.-M. Che and Y. Wang, *Inorg. Chem.*, 1993, **32**, 2518.
- 14 J. A. Bailey, V. M. Miskowski and H. B. Gray, *Inorg. Chem.*, 1993, **32**, 369.
- 15 D. K. Crites, C. T. Cunningham and D. R. McMillin, *Inorg. Chim. Acta*, 1998, **273**, 346.
- 16 M. Weiser-Wallfaher and G. Z. Gliemann, *Z. Naturforsch., Teil B*, 1990, **45**, 652.
- 17 W. B. Connick, L. M. Henling, R. E. Marsh and H. B. Gray, *Inorg. Chem.*, 1996, **35**, 6261.
- 18 D. S. Martin, in *Extended Interactions between Metal Ions*, ed. L. V. Interrante, *ACS Symp. Ser. 5*, American Chemical Society, Washington, DC, 1974, p. 254.
- 19 V. M. Miskowski and V. H. Houlding, *Inorg. Chem.*, 1989, **28**, 1529.
- 20 R. A. Rader, D. R. McMillin, M. T. Buckner, T. G. Matthews, D. J. Casadonte, R. K. Lengel, S. B. Whittaker, L. M. Darmon and R. E. Lyttle, *J. Am. Chem. Soc.*, 1981, **102**, 5906.
- 21 G. Blasse and B. C. Grabmeier, in *Luminescent Materials*, Springer-Verlag, New York, 1994, ch. 3.
- 22 L. Carlsen, H. Egsgaard and J. R. Anderson, *Anal. Chem.*, 1979, **51**, 1593.
- 23 D. D. Perrin, W. L. F. Armarego and D. R. Perrin, *Purification of Laboratory Chemicals*, Pergamon, New York, 2nd edn., 1980.
- 24 F. Liu, K. L. Cunningham, W. Uphues, G. W. Fink, J. Schmolt and D. R. McMillin, *Inorg. Chem.*, 1995, **34**, 2015.
- 25 G. M. Sheldrick, SADABS, A program for absorption corrections with the Siemens SMART system, University of Göttingen, 1996.
- 26 G. M. Sheldrick, SHELX-93, A program for crystal structure refinement, University of Göttingen, 1993.

Paper 8/07914E